Epilepsy Research (2012) **98**, 223—231

journal homepage: www.elsevier.com/locate/epilepsyres

Association between equivalent current dipole source localization and focal cortical dysplasia in epilepsy patients

Alejandro Blenkmann[a,b,c,d,*], **Gustavo Seifer**[a,b], **Juan Pablo Princich**[a,b,d], **Damian Consalvo**[a,b], **Silvia Kochen**[a,b,d], **Carlos Muravchik**[c]

[a] *IBCN ''Dr. E. de Robertis'', School of Medicine, University of Buenos Aires, Paraguay 2155 (1121), Ciudad Autónoma de Buenos Aires, Argentina*
[b] *Department of Neurology, Ramos Mejía Hospital, Urquiza 609 (1221), Ciudad Autónoma de Buenos Aires, Argentina*
[c] *LEICI, School of Engineering, National University of La Plata, Calle 1 esquina 47 (1900), La Plata, Argentina*
[d] *National Scientific and Technical Research Council (CONICET), Ciudad Autónoma de Buenos Aires, Argentina*

Received 15 March 2011; received in revised form 22 September 2011; accepted 26 September 2011
Available online 21 October 2011

KEYWORDS
Focal cortical dysplasia;
Equivalent current dipole;
Magnetic resonance imaging;
Inverse problem;
Epileptogenic zone

Summary We analysed the association between focal cortical dysplasia (FCD) visible in MRI and the location of equivalent current dipole (ECD) of single interictal scalp EEG spikes (IIS) in 11 epilepsy patients. We calculated several indicators of distance of ECDs to the FCD border. The results confirm some previous studies suggesting that the epileptogenic zone associated to the location of ECDs extends beyond the FCD visible in MRI. The analysis suggests the ECDs to be in a shell parallel to part of the FCD surface.
© 2011 Elsevier B.V. All rights reserved.

Introduction

We analysed the association between the localization of focal cortical dysplasia (FCD) and epileptic neural sources modelled by equivalent current dipoles (ECD). FCD, first described in (Taylor et al., 1971), are malformations of cortical development, associated with phenotypic cellular abnormalities that may be the result of abnormal differentiation and/or proliferation. Several studies reported that FCD are intrinsically epileptogenic and that most patients often present drug resistant epilepsy (Mattia et al., 1995; Morioka et al., 2009; Bast et al., 2004; Palmini et al., 2004; Widjaja et al., 2008; Lerner et al., 2009; Palmini, 2010). Resective surgery is frequently a promising therapy in this population. However, the outcome following surgical treatment of these patients has been less successful than in other pathologies such as hippocampal sclerosis, even if the entire magnetic resonance images (MRI) visible lesion is removed (Rosenow and Lüders, 2001; Lerner et al., 2009). The surgical failure in

* Corresponding author at: IBCN ''Dr. E. de Robertis'', School of Medicine, University of Buenos Aires, Paraguay 2155 (1121), Ciudad Autónoma de Buenos Aires, Argentina. Tel.: +54 11 5950 9626; fax: +54 11 5950 9626.
E-mail address: ablenkmann@gmail.com (A. Blenkmann).

0920-1211/$ — see front matter © 2011 Elsevier B.V. All rights reserved.
doi:10.1016/j.eplepsyres.2011.09.018

these patients may be due to the presence of a more extensive, non-MRI visible, epileptogenic FCD (Widdess-Walsh et al., 2006). The key for the success of surgical treatment is the accurate definition of the ''epileptogenic zone'' (EZ), the area of cortex that is indispensable for the generation of epileptic seizures (Chauvel et al., 1987; Rosenow and Lüders, 2001). Today the gold-standard method to define the EZ is the intracranial recording, an invasive procedure that increases morbidity and mortality. In addition, it demands an important amount of materials and human resources. These facts reduce the number of patients undergoing epilepsy surgery, which is below the number of cases for whom it is indicated. This situation is especially notorious in developing countries. In this scenario, non-invasive studies to define EZ are highly desirable (Radhakrishnan, 2009).

The study of the EZ involves the ''irritative zone'' (IZ), the area of cortex responsible for the scalp electroencephalography (EEG) interictal spikes (IIS). Both of these zones are also related to the onset zone of seizures (Chauvel et al., 1987; Rosenow and Lüders, 2001). IIS neural sources can be located solving the so-called inverse problem with an ECD model. The ECD based on scalp EEG is the most often used model for non-invasively estimating the source of cerebral activity, specially to localize the origin of IIS activity (Michel et al., 2004; Ebersole and Hawes-Ebersole, 2007; Plummer et al., 2008). The ECD model assumes that the electromagnetic source in the brain is constrained to a cortical area of small size compared to its depth, i.e. to its radial distance to the scalp. The application of this model in patients with epilepsy and FCD was reported in (Bast et al., 2004; Gavaret et al., 2009) using EEG and (Otsubo et al., 2001; Bast et al., 2004; RamachandranNair et al., 2007; Widjaja et al., 2008) using magnetoencephalography (MEG).

This study aims to validate, in the pre-surgical evaluation of epilepsy patients with FCD, the association between the diagnosed lesion visible in MRI and the relative spatial distribution of ECDs as sources localized from single IIS, using 64 channel scalp EEG.

Materials and methods

The association between the neural sources of IIS and the FCD visible lesions in MRI was performed according to a sequence of operations shown in Fig. 1 in the form of a data flow diagram. The upper part describes the procedure to obtain the ECDs co-registered to FCDs, as calculated with the procedure of the lower branches of the diagram. The following subsections describe all the steps involved.

Patients selection

Patients were evaluated prospectively at the Epilepsy Center of the Ramos Mejía Hospital between 2007 and 2009 using our institutional protocol for the diagnosis of epilepsy (Kochen et al., 2002). A group of 15 patients with drug resistant epilepsy (Kwan et al., 2010) and diagnosis of FCD was selected according to the recent clinicopathological classification of FCD (Blümcke et al., 2011). The patients included were assumed to be FCD Type I or II and those that evidenced an associated pathology, i.e. FCD Type III, were excluded from the study.

Patients had a comprehensive evaluation of history and neurological examination, neuropsychological testing, routine MRI and standard EEG recording. The collected data about ictal semiology was considered with regards to patient and relatives' history, sex, age at seizure onset, seizure types according to International League Against Epilepsy (ILAE) classification 1981, response to treatment and frequency of seizures (Commission on Classification and Terminology of the ILAE, 1981; Kwan et al., 2010).

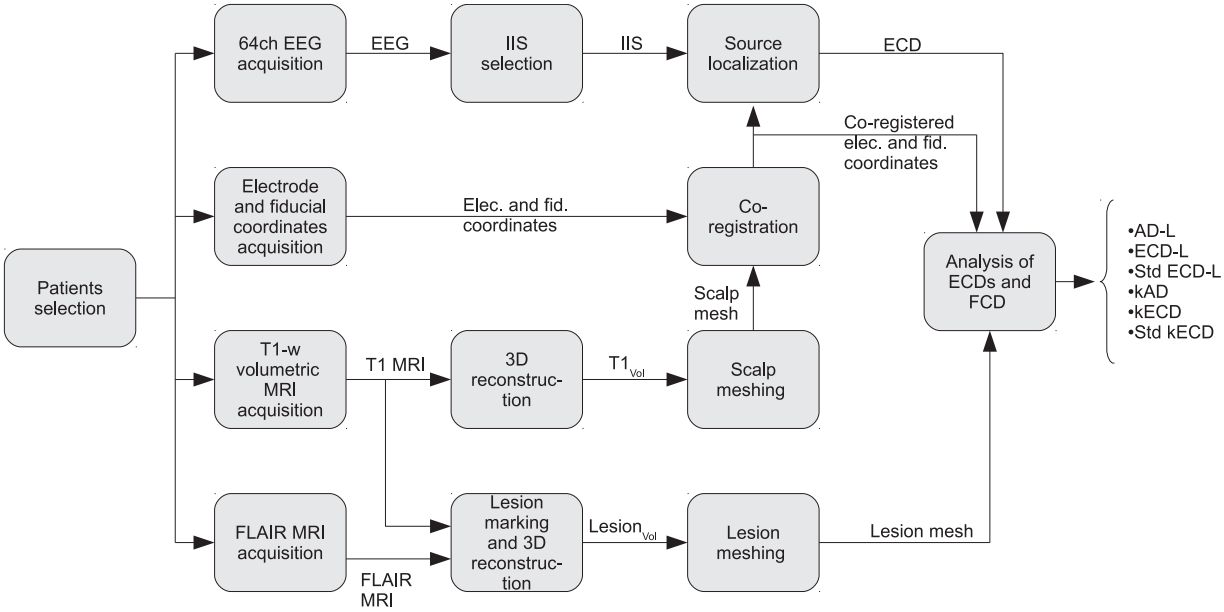

Figure 1 Data flow diagram depicting the sequence of operations performed to obtain equivalent current dipoles (ECD) from interictal spikes (IIS) and study its association with focal cortical dysplasia (FCD) visible lesions in MRI. The boxes represent processing steps and the lines the obtained data.

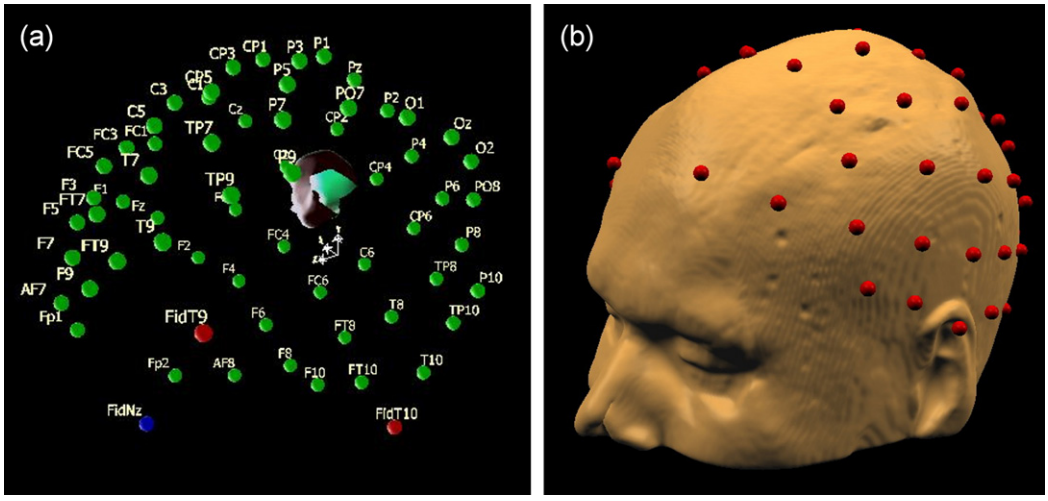

Figure 2 (a) 3D plot of electrodes (in green) and of three fiduciary landmarks (nasion in blue, right and left tragi in red) in a 3D virtual space in 3D Electrode Acquisition. (b) Electrodes and fiducials fitted over the mesh surface of the head using BrainVoyager 2000. (For interpretation of the references to color in this figure legend, the reader is referred to the web version of the article.)

All patients met conventional MRI criteria suggesting FCD including gyration anomalies, focal thickenings of the cortex, blurring of the grey—white matter junction, and abnormal cortical and subcortical signal intensity or transmantle characteristics (Barkovich and Kuzniecky, 1996).

The study was approved by the research ethics committee of the Ramos Mejía Hospital. Patients (and parents) gave their informed consent accepting the procedures in this study and the use of the information.

EEG and electrode positions acquisition

We recorded high resolution EEG (HR-EEG) data from each patient with a 64-channel amplifier Bioscience EEG64 (Bioscience SRL, Argentina). Hardware filter frequency bandpass was 0.5—70 Hz (—3 dB) and sampling rate was set to 200 Hz. Harmonie 5.2 software (Stellate Systems Inc., Canada) was used to acquire data. Scalp electrodes were mounted on an Electro-cap according to the international 10-10 system of electrode placement (including F9/10, FT9/10, T9/10, TP9/10 and P9/10) (Bio-Logic Systems Corp, USA). Recordings were referenced to average mastoidal electrodes. During acquisition sessions, patients were relaxed and asked to lie down with closed eyes for 2—3 h.

Before EEG recording started, we registered spatial coordinates of all electrodes and of three fiduciary landmarks (nasion, right and left tragi) with a three-dimension digitizer system PATRIOT (Polhemus, USA) and 3D Electrode Acquisition software developed by our group (San Martín et al., 2007). Two position sensors were used, namely a primary pen type sensor to acquire electrode and fiduciary points and a secondary sensor, fixed to the cap, as a position reference. The secondary sensor was used to mitigate measurement errors due to unavoidable head movements during the long acquisition procedure. After acquiring all electrode and fiducial positions, our software showed all the points on a 3D plot (Fig. 2) and a simple visual inspection was made to check that digitalized positions were correct. In addition, the software provided a self-validation procedure to check, among other features, for admissible electrode position variance.

Image acquisition and processing

In a second instance, patients were scanned with the same 1.5 T MRI unit (Intera, Philips Medical Systems, Best, Netherlands). The acquired images were structural high-resolution 3D, T1-weighted spoiled gradient recovery volume (TR/TE/TI = 9.2/4.2/450 ms, matrix 256 × 256, bandwidth 31.2 kHz, field of view 256 mm × 256 mm, slice thickness 1 mm) with a final isotropic resolution of 1 mm. Depending on head sizes, approximately 160 slices in the axial plane were acquired and stored in DICOM format. Then, a 3D volume reconstruction, designated $T1_{Vol}$ from now on, was made of each patient head using MRIcron software (Chris Rorden's MRIcron, USA) in NIfTI format. A high resolution mesh of 32768 triangles of the scalp surface was subsequently constructed from this volume using an iterative morphing algorithm in BrainVoyager2000 software (Brain Innovation, The Netherlands).

In addition, all subjects were scanned with a 2D fluid attenuated inversion recovery (FLAIR) sequence (TR/TE/TI = 10,000/147/2200 ms, matrix 192 × 256, bandwidth 15.6 kHz, field of view 240 mm × 240 mm, slice thickness between 4 and 5 mm, no gap) in the coronal and axial planes. The integrity of white matter tracts was also evaluated by means of diffusion tensor imaging (DTI) MRI (Princich et al., 2010).

Lesion marking and processing

The more sensitive FLAIR sequence overlaid into the high resolution T1 were mainly used to depict the shape and location of the lesion, see Fig. 3. Using a volume of interest (VOI) pen tool in MRIcron, an experienced neuroradiologist (J.P.P.) marked the voxels corresponding to the suspected FCD on each slice (axial, sagittal and coronal) according to

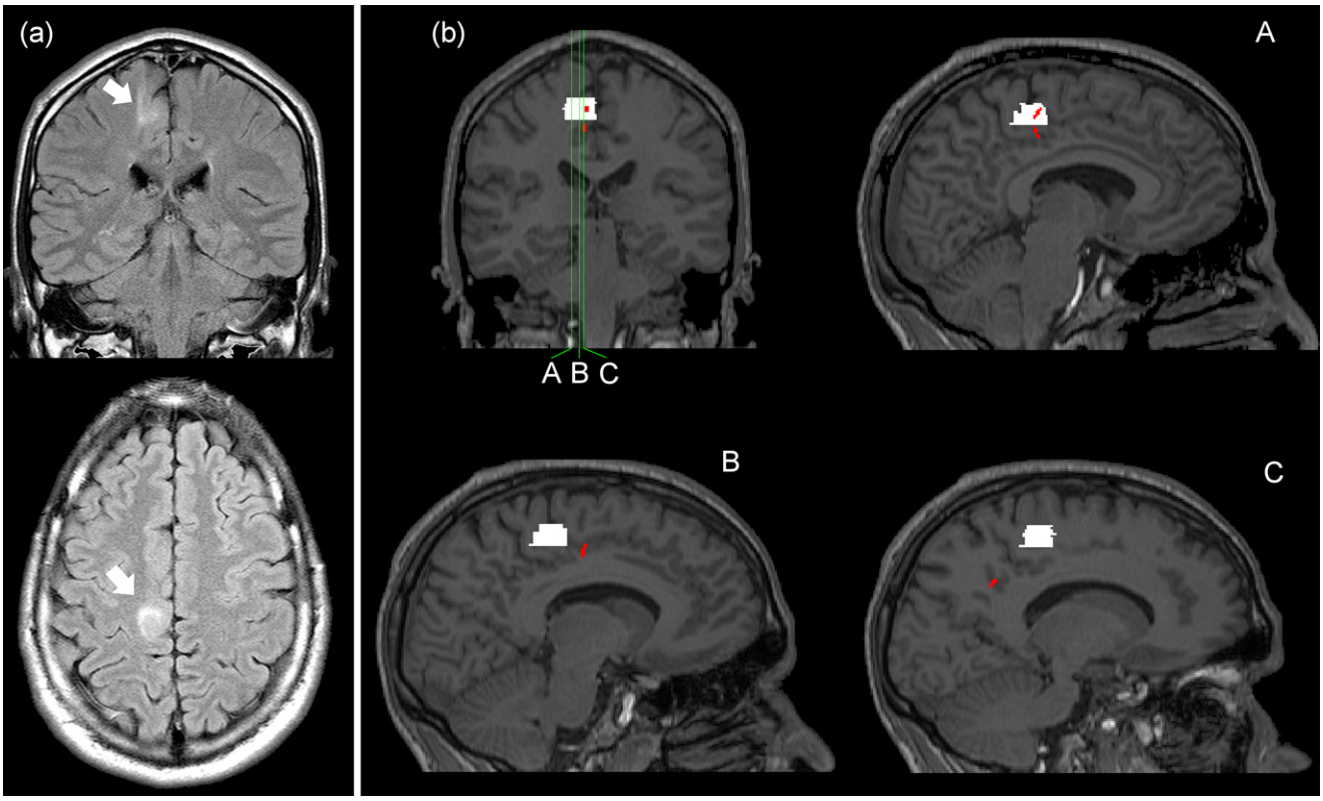

Figure 3 Focal cortical dysplasia (FCD) and equivalent current dipoles (ECD) in patient number 1. MRI images are in radiological convention (LAS). (a) Right frontal FCD on axial and coronal FLAIR images (see white arrows). (b) ECD locations from single IIS (in red) and FCD (in white) overlaid on coronal and sagittal T1 images. Coronal image shows the position of 3 sagittal slices A, B and C. (For interpretation of the references to color in this figure legend, the reader is referred to the web version of the article.)

previously established criteria (Barkovich and Kuzniecky, 1996; Barkovich et al., 2005; Colombo et al., 2009). Thus, we obtained the set of voxels enclosing the anatomical lesion for each subject. These VOIs denoted $Lesion_{Vol}$, were then converted to NIfTI format in the same coordinate system as $T1_{Vol}$. Finally, using Matlab (The MathWorks, USA), a surface mesh describing the lesion border was constructed and its center of mass was calculated.

Registration of electrodes and fiducials with MRI

The electrode position coordinate system needs to be co-registered with $T1_{Vol}$ and $Lesion_{Vol}$ space. For that purpose, we marked fiduciary landmarks on the scalp mesh surface and fitted the electrode coordinates to lay on the mesh, via a rigid body transformation in BrainVoyager2000, see Fig. 2. Fiduciary points were constrained to depart no further than 3 mm from the original position during the fitting procedure to avoid unfeasible electrode locations.

Selection of IIS

A trained neurophysiologist (G.S.) according to IFSECN criteria (Chatrian et al., 1974) visually identified and selected IISs (interictal spikes or spike and waves or sharp waves) based on negative phase reversals on bipolar montages. All the IISs selected had similar morphology and same scalp potential distribution. Afterwards, IISs were extracted in epochs of 400 ms (200 ms before and after the highest amplitude) and loaded into Matlab. We defined ''spike interval'' as the signal having more than 50% of the maximum power in the IIS epoch. The rest of the epoch was defined as ''background activity interval''. Finally, *SNR* of every single IIS was calculated as the mean power of the spike interval over the mean power of the background activity interval. IISs with *SNR* smaller than 1.5 were discarded. We observe that no IIS data was averaged.

ECD localization of IIS neural sources

IIS epochs were analysed using Source Analysis module of Brain Electrical Source Analysis v5.1 (BESA) software (MEGIS Software GmbH, Germany). A high-pass filter at 3 Hz and a low-pass filter at 40 Hz were applied to all channels. Normally, 2—5 channels having artifacts were excluded. Source localization for each single IIS was obtained solving the inverse problem with an ECD model of fixed location, fixed orientation and time varying amplitude. A four-shell ellipsoidal head model was used to solve the direct problem using the co-registered electrode position information. This model is utilized to compute the electric potential distribution on the scalp and to compare the values at the electrode locations with the actual measurements. Each of the layers in the model was assumed to have a constant value of homogeneous and isotropic conductivity relative to CSF. Thus, scalp,

bone, and brain conductivities were set to 0.3300, 0.0042, and 0.3300 respectively. The ellipsoid axes of the outer shell were determined from the electrode positions over the scalp and the thickness of the layers were taken as 6.00, 7.00, and 1.00 mm for scalp, bone, and CSF respectively.

We assumed focal epileptogenic sources in these patients therefore, the source localization procedure was set to estimate a single focal source with one ECD. For each IIS the ECD was calculated fitting the zone of maximum energy (approximately $\pm$6 ms from peak). When the first component of the principal component analysis (PCA) of the signal was larger than 90% the dipole was declared valid; when it was less, the IIS was discarded.

The ECD stability was tested using (Gavaret et al., 2004) criteria, i.e. checking that the location of the ECD did not change significantly when solving the inverse problem on smaller parts of IIS maximum energy zone. If the ECD location remained stable in a small and limited cortex area on a period of time of 20—30 ms around the peak, that area was defined as the origin of the IIS activity. If ECD location changed among distant structures, this revealed that an inadequate source model was used (Gavaret et al., 2009).

When localizing ECD, it is customary to use a goodness of fit (*GoF*) as a measure of the estimation quality (Bast et al., 2006; Gavaret et al., 2004). In this work a threshold of 60% was used to validate or reject an ECD estimate from an IIS.

Analysis of ECDs and FCD

Using the co-registration information, we overlaid in the same space ECDs, $T1_{Vol}$, and lesion surface mesh in Matlab. We devised and calculated several different indicators with the objective of measuring the performance of source localization when comparing source with hypothetical epileptogenic lesion locations. First, from all ECDs of a single individual, an average dipole (AD) was defined, with the average location and orientation. Then, in terms of spatial distance to the MRI lesion, two indicators were measured: the distance from the AD to the lesion border (*AD-L*, column 3 in Table 2) and the mean of the distance from each ECD to the lesion border (*ECD-L*, column 5 in Table 2). To calculate the distance of each ECD to the lesion, positive values of distance were used for ECDs located outside the FCD and negative values otherwise. Individual ECD dispersion (*Di*, column 4 in Table 2) was calculated as the mean distance of each ECD to the AD. The smaller this value is, the higher is the concentration of dipoles about AD. Standard deviation from *ECD-L* (*Std ECD-L*, column 6 in Table 2) and the volume of the diagnosed FCD (column 10 in Table 2) were also measured.

It is interesting to note that ECD estimation was also performed using MUSIC procedure (Mosher et al., 1992) and the results do not differ significantly from those obtained with BESA (Blenkmann et al., 2009).

In order to have a measure of the ECDs location and dispersion relative to the size, location and geometrical characteristics of the FCDs, we defined a scale factor *k* for each ECD. This *k* was calculated as a scale factor that radially expands or contract the FCD surface mesh until it reaches the ECD. A scale factor *k* bigger than one implies the ECD is outside of the FCD, whereas *k* less than one implies the ECD

Table 1 Clinical patient data.

Patient	Gender/age	1st seizure	Medical history	Seizures per month	FCD location in MRI	Transmantle	Hemisphere	Ictal semiology
1	M/29	9 y	No	1.5	F medial gyrus	No	R	Motor SPS
2	F/23	4 y	No	10	F perirolandic	Yes	R	GTCS
3	F/26	2 y	Febrile Seizure	5	Parahippocampus	No	L	Auditive SPS
4	M/31	6 m	Perinatal Infection	0.5	TO	No	L	CPS→ GTCS
5	M/32	4 y	Prolonged labor	0.5	F superor-medial	No	L	Motor SPS→ GTCS
6	M/33	16 y	No	2.5	F central	Yes	R	CPS→ CPC→ CTCG
7	M/29	5 y	No	1	F middle gyrus	Yes	R	Motor SPS
8	M/27	4 y	No	3	F media and superior	Yes	R	Fear→ hypermotor seizure
9	F/15	14 y	No	2	F precentral	Yes	L	CPS→ GTCS
10	M/32	5 m	Hypoxia	15	F anterior	No	R	GTCS
11	F/9	2 m	No	3	FP posterior	No	R	Motor SPS→ GTCS

References: FCD: focal cortical dysplasia, *M*: male, F: female, y: years, m: months, F: frontal, T: temporal, TO: temporo-occipital, FP: fronto-parietal, L: left, R: right. SPS: simple partial seizure, CPS: complex partial seizure, GTCS: generalized tonic—clonic seizure.

Table 2 Equivalent current dipoles (ECD) localization results and measurements relative to diagnosed focal cortical dysplasia (FCD).

Patient	ECD	AD-L [mm]	Di [mm]	ECD-L [mm]	Std ECD-L [mm]	kAD	kECD	Std kECD	Lesion volume [cm^3]	Mean SNR
1	4	4.63	12.96	7.55	10.37	1.91	2.17	1.64	2.18	2.80
2	34	3.97	13.04	13.29	8.14	1.76	3.19	1.34	2.81	4.20
3	4	3.10	27.47	10.99	6.45	–	–	–	4.21	2.59
4	7	13.57	12.32	16.57	7.52	1.83	1.98	0.47	27.49	3.74
5	9	25.09	16.78	28.17	13.99	3.71	4.28	1.54	10.60	3.24
6	5	1.41	18.49	9.46	4.74	1.39	2.20	0.72	7.53	3.97
7	10	22.90	14.22	25.56	12.98	4.56	5.06	2.04	1.83	5.67
8	12	57.44	14.93	59.53	9.74	8.91	9.05	1.18	2.11	2.81
9	12	19.44	7.23	20.89	3.03	3.38	3.27	0.41	8.32	5.45
10	8	4.72	17.29	6.27	9.22	1.24	1.24	0.40	115.74	5.21
11	3	4.66	28.85	20.96	12.80	1.60	3.06	1.40	8.74	2.09
Mean	9.82	14.63	16.69	19.93	9.00	3.03	3.55	1.11	17.41	3.80

References: AD-L: average dipole to lesion distance, *Di*: dispersion, *ECD-L*: mean of all equivalent current dipole to lesion distance, *Std ECD-L*: standard deviation of *ECD-L*, *kAD*: scale factor *k* for average dipole, *kECD*: mean value of scale factor *k* for all equivalent current dipoles, *Std kECD*: standard deviation of *kECD*, *SNR*: signal to noise ratio.
For details explaining indicators, see section ''*Materials and methods*''.

is inside the FCD. In addition, using the same procedure we calculated a scale factor *k* for each AD (*kAD*, column 7 in Table 2), the mean *k* for ECDs (*kECD*, column 8 in Table 2), and the standard deviation of *k* for the ECDs (*Std kECD*, column 9 in Table 2). The main difference between the scale factor *k* and *ECD-L* is that the first measures the distance Lesion-to-ECD relative to the size of the lesion, whereas *ECD-L* measures this distance in absolute terms, regardless of the lesion size. In this way, a mean value of *k* larger than one and a dispersion of *k* smaller than the mean of $k-1$ suggests a thin shell containing the dipoles, parallel to a part or parts of the FCD border. Although the idea behind the *ECD-L* was similar, both measures *ECD-L* and *k* differ slightly. This is particularly so when dipoles are located close to protuberances of the FCD.

Results

From the 15 included patients, 4 were excluded from the study because no IIS were registered or the inclusion criteria were not accomplished. From now on we will refer to the remaining 11 patients as the analysed population.

Mean age of our population was 26 years (9—33 years), 4/7 female/male, they all had a negative family history of epilepsy. Past medical history before epilepsy onset was relevant for 4/11 patients. All patients had normal developmental milestones, except patient number 10 that presented developmental delay. Table 1 summarizes the patients' data.

All IISs accomplishing the inclusion criteria were localized with an ECD. In Table 2 we summarize the localization analysis for each patient. A mean of 9 ECDs for each subject were found (minimum 3 and maximum 34). The overall-mean distance between AD to lesion border was 14 mm and in 6 cases (54%) it was less than 5 mm. Dispersion of ECD varied between 7 and 28 mm, with a mean of 16 mm. In all cases AD were located outside the lesion.

As an example of the results obtained, in Fig. 3 we show patient number 1 T1 and FLAIR images, with the marked FCD and estimated ECDs overlaid.

Patient number 3 had multiple disjoint FCD regions, thus *kAD*, *kECD*, *Std kECD* were undefined for this kind of FCD and were not included in Table 2.

Note that for all patients but two (numbers 1 and 10), the *ECD-L* is larger than the *Std ECD-L*. This seems to show that the dipoles are significantly outside the FCD. When analysing *kECD* and *Std kECD* the conclusions are similar.

Discussion

The aim of this work was to analyse the association between FCD visible in MRI and the spatial distribution of ECDs estimated from solving the inverse problem for single IIS. In order to achieve this objective we marked the visible lesions in MRI and measured different indicators describing the spatial distribution of ECDs.

As shown in Table 2, *ECD-L* are positive and *Std ECD-L* are less than *ECD-L*, suggesting that ECD are significantly outside FCD and therefore, that IZ extends beyond visible FCD in MRI. This observation is challenged in the case of patients 1 and 10. A similar result is derived given that *kECD* is larger than 1 and *Std kECD* smaller than $kECD-1$ (Fig. 4). Thus, results obtained in this study are in agreement with previous studies. Indeed, several papers have shown that the EZ in cases of FCD is often larger than visible lesion in MRI (Cepeda et al., 2005; Iida et al., 2005; RamachandranNair et al., 2007; Widjaja et al., 2008; Aubert et al., 2009). A hypothesis that could explain this outcome is that MRI allows distinguishing lesional FCD tissue from normal tissue due to the presence of cytomegalic neurons or balloon cells. However, epileptogenic tissue may involve other kind of pacemaker cells (for example, immature neurons) or an epileptogenic network of normal neurons in a feedback loop. This hypothesis is consistent with evidence that histological normal tissue

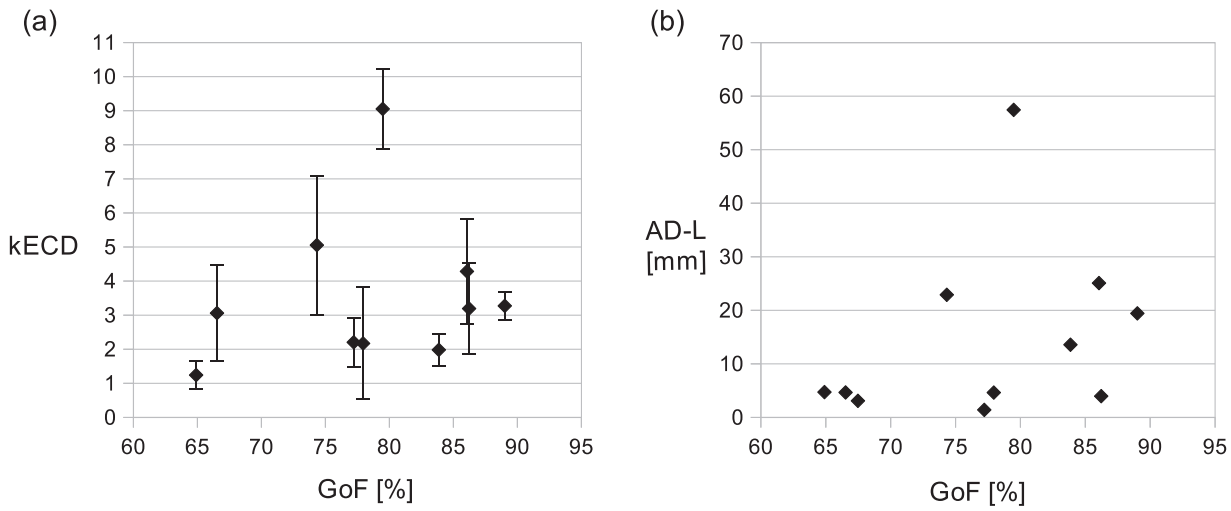

Figure 4 (a) *kECD* against *GoF*. Error bars represent ±*Std kECD*. Note that *kECD* less *Std kECD* is bigger than 1 in all patients but numbers 2 and 8, suggesting that the IZ is outside the FCD. (b) *AD-L* against mean *GoF* for all patients. Note that no significant differences are observed for different values of *GoF*. References: *AD-L*: average dipole to lesion distance, *GoF*: goodness of fit, *kECD*: mean value of scale factor *k* for all equivalent current dipoles, *Std kECD*: standard deviation of *kECD*, *SNR*: signal to noise ratio. For details explaining indicators, see section ''*Materials and methods*''.

(not containing abnormal cells) in patients with FCD, had near normal ECoG recordings in only 22% of the cases, i.e. abnormal ECoG in the other 78% (Cepeda et al., 2005). In the same sense, in a MEG study that included 4 patients with FCD, 3 of them had interictal MEG spike source (MEGSS) clusters that included the MRI lesion and extended contiguously out from it and there were also scattered MEGSS remote from the lesion. The remaining case had scattered MEGSS that included the lesion and contiguously spread out of it (Iida et al., 2005).

Interestingly, we have to note that *AD-L*, *ECD-L*, *kAD* and *kECD* in patient number 8 are relatively large compared with other patients. Also, patient numbers 2 and 8 had 10 and 12 IIS of another type respectively, that were different in signal morphology and in scalp potential distribution from those analysed previously. ECD analysis for these IIS resulted in remote locations from the visible lesion. In these cases, EZ might be associated to FCD and remote (extralesional) structures in a network organization, as in (Aubert et al., 2009). These authors studied patients with epilepsy and FCD, and distinguished remote and local epileptogenic sources using ECoG. Twenty-two out of thirty-six (61%) of their patients had a network EZ organization involved in the seizure onset. In these cases, complete resection of the EZ (including remote locations) had a better outcome than incomplete resection. Similar results were found in (Fauser et al., 2009). This result and the previous ones reinforce the hypothesis that EZ may be organized as networks that span from visible FCD in MRI and also beyond the limits of the lesion, or to more remote zones.

In contrast to the work mentioned above, other studies showed that source localization of IIS from EEG and MEG are principally located within the visible lesion in MRI (Morioka et al., 2009; Bast et al., 2004). In Bast et al., 122 channels MEG and 33 channels EEG were used to localize IIS. A 92.5% *GoF* threshold criteria was used to exclude ECD, rejecting 40% of the EEG IIS, resulting in a 93% of the ECD located within the FCD. If such a threshold was applied to our data, almost all of the IIS would be rejected (Fig. 4). Yet, if we only considered the best 4 cases of *GoF*, over 83%, it can be seen from Fig. 4 that no different conclusion about *AD-L* can be drawn from the set of 6 patients *GoF* less than 83%. A similar conclusion arises when observing the other indicators introduced in this paper.

We remind that a low *GoF* measures how much of the measured data is explained by the model. A conjecture to explain low *GoF* in our study is the simultaneous presence of substantial background activity (i.e. activity from other parts of the brain that is not related to the FCD) and IIS. A technique with some degree of spatial filtering, as in (Beltrachini et al., 2009), could be applied to reduce the amount of cluttering background activity. This will be the subject of forthcoming work. Another conjecture is that the extension of the source is too large, making an ECD a bad source model and thus reducing the *GoF* (Bast et al., 2006; Tao et al., 2007). In these cases, fitting an extended source model (Yetik et al., 2006) seems advisable. Other possible difference with (Bast et al., 2004) is due to population age, which were mostly children and adolescent patients as opposed to mainly adults in our study.

We have to remark that the relevance of ECD locations, i.e., if they correctly estimate the EZ, will be finally determined by invasive recordings and/or post surgical outcome. It has been shown from intracranial recordings that complete resection of ictal onset zone and interictal zone significantly increase post-surgical seizure freedom (Widdess-Walsh et al., 2007). However, IZ are not always wholly contained within EZ and therefore, the resection of an IZ outside EZ may not affect surgical outcome.

In spite of the best efforts made, the correct placement of intracranial electrodes in patients with FCD is not always achieved. It has been reported that observing diffuse or spread-like epileptogenic patterns from neural sources distant to the electrodes or in deep locations, significantly

decreases post-surgical success (Widdess-Walsh et al., 2007). In these situations, non-invasive ECD localization of IIS may provide an interesting approach. Assuming that ECD neural sources are the same that would be found from intracranial recordings, this information may assist in planning intracranial electrode placement and/or surgical resection.

Additional attention must be paid to spread ECDs when some sources of activity extend beyond the FCD visible in MRI. These spread-like sources may include dormant regions that could rekindle after the resection of what appears to be the EZ, leading to future seizure recurrence.

In summary, our findings suggest that the FCD visible in MRI and cortex areas nearby it are epileptogenic, which agrees with previous studies. The method described here, based on scalp EEG and MRI, is useful to define the extension of the IZ in patients having epilepsy and FCD visible in MRI, and could be applied in the study of other focal pathologies associated with epilepsy. Consideration of ECD localization from single IIS may be helpful to improve the successful outcome of resective surgery.

Acknowledgements

This work was supported by grants from ANPCyT PICT 2005-35423 and PICT 2007-00535, UNLP 11-I-127 all from Argentina. SK, JPP and AB are also supported by CONICET and CM by CIC-PBA.

References

Aubert, S., Wendling, F., Regis, J., McGonigal, A., Figarella-Branger, D., Peragut, J., Girard, N., Chauvel, P., Bartolomei, F., 2009. Local and remote epileptogenicity in focal cortical dysplasias and neurodevelopmental tumours. Brain 132, 3072—3086.

Barkovich, A.J., Kuzniecky, R.I., 1996. Neuroimaging of focal malformations of cortical development. J. Clin. Neurophysiol. 13, 481—494.

Barkovich, A.J., Kuzniecky, R.I., Jackson, G.D., Guerrini, R., Dobyns, W.B., 2005. A developmental and genetic classification for malformations of cortical development. Neurology 65, 1873—1887.

Bast, T., Oezkan, O., Rona, S., Stippich, C., Seitz, A., Rupp, A., Fauser, S., Zentner, J., Rating, D., Scherg, M., 2004. EEG and MEG source analysis of single and averaged interictal spikes reveals intrinsic epileptogenicity in focal cortical dysplasia. Epilepsia 45, 621—631.

Bast, T., Boppel, T., Rupp, A., Harting, I., Hoechstetter, K., Fauser, S., Schulze-Bonhage, A., Rating, D., Scherg, M., 2006. Noninvasive source localization of interictal EEG spikes: effects of signal-to-noise ratio and averaging. J. Clin. Neurophysiol. 23, 487—497.

Beltrachini, L., Ellenrieder, N.V., Muravchik, C.H., 2009. Estimador regularizado de la matriz de covarianza y su aplicación en el análisis del problema inverso en EEG mediante beamforming. In: Proc. of XIII Reunión de Trabajo en Procesamiento de la Información y Control, Rosario, Argentina, 16—18 September, pp. 351—356.

Blenkmann, A., Ellenrieder, N.V., Seifer, G., Princich, J.P., Kochen, S., Muravchik, C.H., 2009. Algoritmo MUSIC para la localización de fuentes de actividad cerebral. Simulación y ejemplos. In: Proc. of XVI Congreso Argentino de Bioingeniería (SABI 2009), Rosario, Argentina, October 14—16, p. 175.

Blümcke, I., Thom, M., Aronica, E., Armstrong, D.D., Vinters, H.V., Palmini, A., Jacques, T.S., Avanzini, G., Barkovich, A.J., Battaglia, G., Becker, A., Cepeda, C., Cendes, F., Colombo, N., Crino, P., Cross, J.H., Delalande, O., Dubeau, F., Duncan, J., Guerrini, R., Kahane, P., Mathern, G., Najm, I., Ozkara, C., Raybaud, C., Represa, A., Roper, S.N., Salamon, N., Schulze-Bonhage, A., Tassi, L., Vezzani, A., Spreafico, R., 2011. The clinicopathologic spectrum of focal cortical dysplasias: a consensus classification proposed by an ad hoc task force of the ILAE diagnostic methods commission. Epilepsia 52, 158—174.

Cepeda, C., André, V.M., Flores-Hernández, J., Nguyen, O.K., Wu, N., Klapstein, G.J., Nguyen, S., Koh, S., Vinters, H.V., Levine, M.S., Mathern, G.W., 2005. Pediatric cortical dysplasia: correlations between neuroimaging, electrophysiology and location of cytomegalic neurons and balloon cells and Glutamate/GABA synaptic circuits. Dev. Neurosci. 27, 59—76.

Chatrian, G., Bergamini, L., Dondey, M., Klass, D., Lennox-Buchthal, M., Petersen, I., 1974. A glossary of terms most commonly used by clinical electroencephalographers. Electroencephalogr. Clin. Neurophysiol. 37, 538—548.

Chauvel, P., Buser, P., Badier, J.M., Liegeois-Chauvel, C., Marquis, P., Bancaud, J., 1987. The epileptogenic zone in humans: representation of intercritical events by spatio-temporal maps. Rev. Neurol. (Paris) 143, 443—450.

Commission on Classification and Terminology of the International League Against Epilepsy [ILAE], 1981. Proposal for revised clinical and electroencephalographic classification of epileptic seizures from the commission on classification and terminology of the International League Against Epilepsy. Epilepsia 22, 489—501.

Colombo, N., Salamon, N., Raybaud, C., Ozkara, C., Barkovich, A.J., 2009. Imaging of malformations of cortical development. Epileptic. Disord. 11, 194—205.

Ebersole, J.S., Hawes-Ebersole, S., 2007. Clinical application of dipole models in the localization of epileptiform activity. J. Clin. Neurophysiol. 24, 120—129.

Fauser, S., Sisodiya, S.M., Martinian, L., Thom, M., Gumbinger, C., Huppertz, H., Hader, C., Strobl, K., Steinhoff, B.J., Prinz, M., Zentner, J., Schulze-Bonhage, A., 2009. Multi-focal occurrence of cortical dysplasia in epilepsy patients. Brain 132, 2079—2090.

Gavaret, M., Badier, J.M., Marquis, P., Bartolomei, F., Chauvel, P., 2004. Electric source imaging in temporal lobe epilepsy. J. Clin. Neurophysiol. 21, 267—282.

Gavaret, M., Trébuchon, A., Bartolomei, F., Marquis, P., McGonigal, A., Wendling, F., Regis, J., Badier, J., Chauvel, P., 2009. Source localization of scalp-EEG interictal spikes in posterior cortex epilepsies investigated by HR-EEG and SEEG. Epilepsia 50, 276—289.

Iida, K., Otsubo, H., Matsumoto, Y., Ochi, A., Oishi, M., Holowka, S., Pang, E., Elliott, I., Weiss, S.K., Chuang, S.H., Snead, O.C., Rutka, J.T., 2005. Characterizing magnetic spike sources by using magnetoencephalography-guided neuronavigation in epilepsy surgery in pediatric patients. J. Neurosurg. 102, 187—196.

Kochen, S., Giagante, B., Consalvo, D., Oddo, S., Silva, W., Solis, P., Centurion, E., Saidon, P., 2002. Analisis retrospectivo (1984—2000). Experiencia en pacientes candidatos a cirugía de la epilepsia. Rev. Neurol. Arg. 27, 41—44.

Kwan, P., Arzimanoglou, A., Berg, A.T., Brodie, M.J., Hauser, W.A., Mathern, G., Moshé, S.L., Perucca, E., Wiebe, S., French, J., 2010. Definition of drug resistant epilepsy: consensus proposal by the ad hoc Task Force of the ILAE Commission on Therapeutic Strategies. Epilepsia 51, 1069—1077.

Lerner, J.T., Salamon, N., Hauptman, J.S., Velasco, T.R., Hemb, M., Wu, J.Y., Sankar, R., Shields, W.D., Engel, J., Fried, I., Cepeda, C., Andre, V.M., Levine, M.S., Miyata, H., Yong, W.H., Vinters, H.V., Mathern, G.W., 2009. Assessment and surgical outcomes for mild Type I and severe Type II cortical dysplasia: a critical review and the UCLA experience. Epilepsia 50, 1310—1335.

San Martín, J., Laforcada, H., Ellenrieder, N.V., Muravchik, C., Papayannis, C., Kochen, S., 2007. Determinación de la posición de electrodos de electroencefalografíia. In: Proc. of XV Congreso Argentino de Bioingeniería (SABI 2007), San Juan, Argentina, September 26—28, pp. 137—140.

Mattia, D., Olivier, A., Avoli, M., 1995. Seizure-like discharges recorded in human dysplastic neocortex maintained in vitro. Neurology 45, 1391—1395.

Michel, C., Murray, M., Lantz, G., Gonzalez, S., Spinelli, L., Peralta, R.G.D., 2004. EEG source imaging. Clin. Neurophysiol. 115, 2195—2222.

Morioka, T., Nishio, S., Ishibashi, H., Muraishi, M., Hisada, K., Shigeto, H., Yamamoto, T., Fukui, M., 2009. Intrinsic epileptogenicity of focal cortical dysplasia as revealed by magnetoencephalography and electrocorticography. Epilepsy Res. 33, 177—187.

Mosher, J.C., Lewis, P.S., Leahy, R.M., 1992. Multiple dipole modeling and localization from spatio-temporal MEG data. IEEE Trans. Biomed. Eng. 39, 541—557.

Otsubo, H., Ochi, A., Elliott, I., Chuang, S.H., Rutka, J.T., Jay, V., Aung, M., Sobel, D.F., Snead, O.C., 2001. MEG predicts epileptic zone in lesional extrahippocampal epilepsy: 12 pediatric surgery cases. Epilepsia 42, 1523—1530.

Palmini, A., Najm, I., Avanzini, G., Babb, T., Guerrini, R., Foldvary-Schaefer, N., Jackson, G., Lüders, H.O., Prayson, R., Spreafico, R., Vinters, H.V., 2004. Terminology and classification of the cortical dysplasias. Neurology 62 (Suppl. 3), S2—S8.

Palmini, A., 2010. Electrophysiology of the focal cortical dysplasias. Epilepsia 51 (Suppl. 1), 23—26.

Plummer, C., Harvey, A.S., Cook, M., 2008. EEG source localization in focal epilepsy: where are we now? Epilepsia 49, 201—218.

Princich, J.P., Seifer, G., Blenkmann, A., Consalvo, D., Kochen, S., 2010. White matter changes associated with focal cortical dysplasia (FCD) in refractory epilepsy patients detected with diffusion tensor imaging (DTI) in magnetic resonance. In: 6th Latin-American Congress on Epilepsy, Cartagena, Colombia, August 1—4, p. 113.

Radhakrishnan, K., 2009. Challenges in the management of epilepsy in resource-poor countries. Nat. Rev. Neurol. 5, 323—330.

RamachandranNair, R., Otsubo, H., Shroff, M.M., Ochi, A., Weiss, S.K., Rutka, J.T., Snead, O.C., 2007. MEG predicts outcome following surgery for intractable epilepsy in children with normal or nonfocal MRI findings. Epilepsia 48, 149—157.

Rosenow, F., Lüders, H., 2001. Presurgical evaluation of epilepsy. Brain 124, 1683—1700.

Tao, J.X., Baldwin, M., Ray, A., Hawes-Ebersole, S., Ebersole, J.S., 2007. The impact of cerebral source area and synchrony on recording scalp electroencephalography ictal patterns. Epilepsia 48, 2167—2176.

Taylor, D.C., Falconer, M.A., Bruton, C.J., Corsellis, J.A., 1971. Focal dysplasia of the cerebral cortex in epilepsy. J. Neurol. Neurosurg. Psychiatry 34, 369—387.

Widdess-Walsh, P., Diehl, B., Najm, I., 2006. Neuroimaging of focal cortical dysplasia. J. Neuroimaging 16, 185—196.

Widdess-Walsh, P., Jeha, L., Nair, D., Kotagal, P., Bingaman, W., Najm, I., 2007. Subdural electrode analysis in focal cortical dysplasia: predictors of surgical outcome. Neurology 69, 660—667.

Widjaja, E., Otsubo, H., Raybaud, C., Ochi, A., Chan, D., Rutka, J.T., Snead, O.C., Halliday, W., Sakuta, R., Galicia, E., Shelef, I., Chuang, S.H., 2008. Characteristics of MEG and MRI between Taylor's focal cortical dysplasia (Type II) and other cortical dysplasia: surgical outcome after complete resection of MEG spike source and MR lesion in pediatric cortical dysplasia. Epilepsy Res. 82, 147—155.

Yetik, I.S., Nehorai, A., Muravchik, C.H., Haueisen, J., Eiselt, M., 2006. Surface-source modeling and estimation using biomagnetic measurements. IEEE Trans. Biomed. Eng. 53, 1872—8253.